HHS Public Access

Author manuscript

J Pharm Sci. Author manuscript.

Method to Determine Syringe Silicone Oil Layer Heterogeneity and Investigation of its Impact on Product Particle Counts

Michelle Cua[a,1,✉], **Daniel Martin**[a,1,✉], **Patricia Meza**[b], **Gianni Torraca**[b], **Thomas Pearson**[b], **Shawn Cao**[b], **Changhuei Yang**[a]

[a]California Institute of Technology, Electrical Engineering, Pasadena, CA, 91125, USA

[b]Amgen Process Development, Thousand Oaks, CA, 91320, USA

Abstract

Pre-filled syringes (PFSs) are commonly used for parenteral delivery of protein therapeutics. In PFSs, the inner surface of the syringe barrel is typically coated with silicone oil for lubrication. The total amount of silicone oil as well as its distribution can impact syringe functionality and particle formation. However, methods to non-destructively characterize the silicone oil distribution are limited. In this paper, we developed a method to visualize and quantify the relative distribution of silicone oil in unfilled syringes using a custom-built multi-color interferometric imaging system. We then applied the system in a preliminary study to investigate the impact of the silicone oil distribution on the number of particles formed in solution after filling and extrusion for two different types of syringes. The syringe type with significantly lower particle counts also exhibited significantly more homogeneous silicone oil distributions. Within syringe types, no significant association was found between silicone oil distribution and particle formation. Our method can be used in further studies that investigate the impact of syringe siliconization on PFS functionality and particle formation.

Keywords

particle size; drug delivery system(s); image analysis; imaging methods(s); injectables

1. Introduction

Glass prefilled syringes (PFSs) have been increasingly adopted for parenteral drug storage and delivery of therapeutic protein formulations. In comparison to traditional vials, PFSs offer many advantages for drug delivery, such as decreased risk of contamination, improved ease of handling, and increased dosage consistency [1]. To improve the functionality of glass PFSs, the stopper and inner surface of the barrel are often coated with silicone oil that serves

[✉]Corresponding Authors ecua@caltech.edu (Michelle Cua), damartin@caltech.edu (Daniel Martin).

[1]These authors contributed equally to this work.

Declaration of Interests: none

as a lubricant to reduce injection force, ensure smooth injection, and prevent incomplete drug dosage.

Both the total amount of silicone oil as well as its distribution can impact PFS functionality. Insufficient siliconization can lead to stalling [2, 3], whereas excessive siliconization can lead to increased level of particles [4]. Apart from the total amount, the silicone oil distribution also plays an important role for myriad reasons. Mechanically, heterogeneous distributions can result in uneven gliding forces and incomplete drug dispensation [3]. Functionally, the silicone oil distribution may also impact the formation of both sub-visible particles (SbVP) and visible particles. Silicone oil droplets can form from oil sloughed off the coating [2, 5]. The silicone-water interfaces can serve as sites for protein adsorption, which can result in loss of product and increased protein aggregation and particle formation [2, 6, 7]. Uneven oil distributions may thereby impact particle formation by providing a larger interfacial surface area for silicone oil migration and protein interactions [8, 9]. The uneven distribution can also expose areas of glass to the protein formulations, providing yet another interface for protein adsorption and aggregation [10].

Limiting particle formation is important in the design and manufacturing of PFSs due to compliance and product quality reasons. Global pharmacopoeias regulate the number of SbVPs larger than 10μm and 25μm in injectable therapeutic products [11-13]. Although currently unregulated, SbVPs in the range of 0.1 μm to 10μm are of growing interest due to their potential immunogenicity [14, 15].

Currently, pharmaceutical companies fill a batch of syringes with drug product and test the particle counts of a subset as part of product release and stability programs. If the particle counts exceed regulation, a deviation is opened to systematically investigate root causes, determine product quality impact, and if required, generate corrective actions. Based on the outcome of the investigation, actions up to and potentially including batch rejection will be taken as appropriate. This is a very time- and resource- intensive approach. If a correlation between silicone oil distribution in an unfilled syringe and particle counts exists, it could be beneficial in improving quality and reducing waste. Thus, monitoring the silicone oil distribution is important, not only for mechanical functionality, but also for regulatory compliance and economic reasons.

Methods to investigate the silicone oil layer distribution in unfilled PFSs are limited. A common method for measuring oil layer thickness is white-light, thin-film interferometry [8]. Existing instruments measure the silicone oil layer thickness at discrete points and interpolate to get the overall thickness [8]. Thus, these methods require a large amount of sampling to adequately map out the oil topology. Other techniques include confocal Raman spectroscopy, 3D laser scanning microscopy, and the powder method. Confocal Raman spectroscopy determines the presence of silicone oil but not the relative evenness in the distribution [3]. 3D laser scanning microscopy is able to measure the thickness distribution but requires destructive sample preparation [16]. The powder method allows for a rough visualization of the silicone oil layer but is destructive and requires a sufficiently thick silicone oil layer [8]. These methods are challenging to use for routine analysis of the

silicone oil layer distribution due to their long time requirements, limited sensitivity, and/or destructive nature.

As an alternative to direct topological measurements, we developed a technology to non-destructively visualize and quantify the heterogeneity in the oil distribution in unfilled syringes. In contrast to the aforementioned methods, our method is not focused on measuring the oil layer thickness or presence of silicone oil, but in quantifying the relative evenness in the distribution. A multi-color interferometric imaging system was designed to visualize the relative distribution of the silicone oil layer. The heterogeneity in the distribution was quantified from the captured interferograms using two parameters that we developed: the number of spots and the heterogeneity percent. After verifying the system performance, we applied our system in a preliminary study to investigate the impact of the silicone oil distribution on particle formation. As opposed to existing interferometric methods, our method is capable of measuring the relative heterogeneity of the silicone oil layer non-destructively within the full field-of-view of the camera, thereby allowing for greater surface measurement in a shorter time.

2. Materials and Methods

2.1. Syringe Samples

This study used two types of commercially available, 2.25 mL, siliconized, glass syringes (Becton, Dickinson, and Company, NJ, USA). These syringes were siliconized using two different methods: with a fixed nozzle and with a diving nozzle. In this manuscript, these syringes will be referred to as PFS-F (prefilled syringe – fixed nozzle) and PFS-D (prefilled syringe – diving nozzle). The syringes were sealed with a rubber stopper in a clean room and stored needle side up in their original containers.

2.2. Multi-Color Interferometric Imaging System

The multi-color interferometric imaging system that was used to visualize the distribution of silicone oil was built by modifying an inverted, reflected-light microscope (Olympus IX-81). A simplified schematic showing the main components of the optical setup is provided in Figure 1A. The light source consisted of a white LED source (Prior Scientific LDB100F) that was filtered by a three-wavelength bandpass filter (Semrock FF01-457/530/628-25) chosen to match the quantum efficiency of the RGB channels of the camera (The Imaging Source DFK 38UX267).

The light source was transmitted to the syringe by a pair of lens and a beamsplitter. The back-reflected light from the syringe was collected by an objective lens (Olympus LMPLFLN 10x) and relayed to the camera. The detected light contained the interference pattern generated from light back reflected off the oil/glass and oil/air interfaces on the inner aspect of the syringe and thus provided a visualization of the oil distribution.

The imaging system had a lateral resolution of about 1.10μm. To correct for defocus due to the curvature of the syringe, the vertical field of view was reduced; the total area imaged was about 0.6mm by 1.4mm (550 x 1024 pixels).

2.2.1. Syringe Holder—A custom mount was designed to hold the syringes (Fig. 1B,C). The syringe rested on two brass rods which were attached to a rectangular annulus via vertical mounts that extended from the bottom of the plate. The system imaged the inner surface of the syringe through a 4.5 mm gap between the rods.

The rods were connected to each other at one end by a belt system. One of the rods was connected to a motor shaft (Lin Engineering, #208) on the other end. The stepper motor controlled the rotation of the two rods and the syringe.

The syringe holder was designed to sit flush inside a Prior Scientific H117 stage that controlled the lateral position of the syringe. An Olympus UX Hub controlled the vertical height of the objective lens and a separate driver (Lin Engineering R256) controlled the rotation motor. The holder was designed such that each syringe was imaged from the same starting position, which was approximately 7.5mm from the syringe flange.

2.2.2. Imaging Procedure—A software program was written to control the microscope hardware and perform the imaging. The user specified what fraction of the inner surface of the syringe to image. From this user-specified fraction, or percent coverage, the number of angular lines (images at different rotations) and images per line (images along the barrel) were computed to best evenly sample the inner surface of the syringe.

Prior to imaging, the relative height and tilt of the syringe barrel was first determined using an autofocus algorithm. The relative height of the syringe at a specific point was determined by acquiring a series of images with the objective lens positioned at different heights (z-axis position). For each image in the series, a focus metric based on image sharpness [15] was computed to find the most in-focus image.

This autofocus procedure was performed at discrete points along the barrel in order to estimate the tilt in the syringe barrel. To reduce overall imaging time, three test points, evenly distributed from flange to needle end, were chosen per rotation. The autofocus procedure provided a linear estimate of the vertical and horizontal tilt in the syringe. During imaging, this linear model was used to adjust the height of the objective lens relative to the syringe to keep the detected interference patterns in focus.

For imaging, the system first translated the syringe laterally, acquiring images along the barrel. After acquiring a line, the system returned to the starting position and then rotated the syringe to acquire another line. The autofocus procedure was repeated between successive rotations to reduce potential errors due to eccentricities in the syringe's profile. The acquired interference images were saved for further processing to quantify the heterogeneity in the oil distribution.

2.3. Quantification of Oil Distribution Heterogeneity

Two different metrics were developed to quantify the amount of heterogeneity in the silicone oil distribution: the number of spots and the heterogeneity percent.

2.3.1. Number of Spots—The first parameter, the number of spots, quantified the number of dark objects within each interferogram. Objects of low intensity were found at the center of circular fringes (Figure 2A). Quantifying the number of spots in an interferogram could provide an estimate for the amount of heterogeneity in the oil distribution.

Prior to detecting the spots, a calibration image was first used to remove spots that were the result of imperfections or dirt in the imaging system. Then, for every point in the image, the standard deviation within a local 74μm^2 window was computed. Since dark spots are surrounded by fringes, the standard deviation in these areas would be high. The remaining objects were thresholded by size (≥15μm^2), eccentricity (< 0.96), and intensity. Figure 2B shows the automatically detected spots in a sample fringe image.

2.3.2. Heterogeneity Percent—The second parameter, the heterogeneity percent, quantified the amount of gray-scale intensity variation in the image. The color and intensity of an interference pattern depends on the local thickness of the interrogated area. Thus, an interferogram of an evenly distributed oil layer has smaller changes in intensity compared to an interferogram of a more heterogeneous oil distribution. To quantify this, each image was first filtered using a quadrature filter [18] to reduce noise while maintaining the fringe pattern. Next, the image was divided into windows of 75 by 75 pixels, and the standard deviation of the pixel intensities within each window was computed. The heterogeneity percent was determined by computing the fraction of windows that had a standard deviation above a pre-determined threshold. This was reported as the fraction of the image, in percent.

2.4. Particle Counting

The number of SbVPs in the solution was quantified using a Microflow Imaging™ (MFI™) DPA4200 particle analyzer (Protein Simple). After the solution was extruded from the syringe through the needle, it was degassed in a vacuum chamber to remove air bubbles. The MFI™ was then loaded with 1 mL of this degassed, extruded solution. From this 1mL, the particles contained within 0.5-0.6 mL were counted. The MFI™ View Analysis Suite software distinguished counts by radii of 1, 2, 5, 10, 25, and 50μm. Since the MFI™ results indicated that the detected particles were predominantly spherical, all measured particles were assumed to be silicone oil droplets for our analyses.

2.5. Method Development

We first investigated the repeatability and required percent coverage to accurately quantify the silicone oil distribution. For repeatability, an unfilled syringe was imaged five consecutive times at 100% coverage (46 angular lines, 29 images per line). The syringe was re-loaded to a different starting rotation prior to each consecutive repetition.

To determine the impact of percent coverage on the error in estimating the heterogeneity in the silicone oil distribution, 10 unfilled syringes (5 each from PFS-F and PFS-D) were imaged at 100% coverage. For each syringe, the acquired dataset was sub-sampled to simulate a smaller percent coverage. 9 unique sub-sampled datasets were used to estimate the percent error for each percent coverage. The percent error was computed by comparing

the average heterogeneity results calculated from the lower percent coverage to the results from the full coverage.

Lastly, we tested the accuracy of the algorithm used to quantify the number of spots in each image by comparing the results of the algorithm to that of manual, visual inspection. A set of 200 images, randomly sampled from the entire data set, was used for this test.

2.6. Experimental Details

To investigate the association between particle counts and silicone oil distribution heterogeneity, we used a sample of 100, 2.25mL syringes that came from two types of syringes: PFS-F (n = 50) and PFS-D (n = 50).

PFS-D, a newer generation of syringes, was compared to PFS-F. Each syringe was given a unique identifier and imaged at 25% coverage (15 angular lines, 23 images per line). For each acquired image, the two heterogeneity parameters - the number of spots and the heterogeneity percent - were computed, and an average value for each parameter was determined for each syringe.

After imaging, the syringes were filled with a therapeutic protein solution that contained a proprietary antibody formulated with buffer, excipients, and surfactant (polysorbate). The number of particles in the extruded solution was quantified using the MFI™ DPA4200 instrument.

3. Results

3.1. Method Development

To determine the system repeatability, the relative variation in average parameter value was determined by computing the coefficient of variation for the five data sets. The heterogeneity percent had a smaller coefficient of variation (1.1%) in comparison to the number of spots (3.5%). Both quantifiers varied less than 5% relative to their respective means.

We also investigated the impact of sub-sampling the inner surface of the syringe on measuring the heterogeneity (Fig. 3). A larger percent coverage was associated with smaller percent error. The number of spots parameter produced the largest discrepancy from the full coverage value. For the heterogeneity percent, the error from sub-sampling remained below 5%. Overall, the average percent error was below 10% across both parameters when the inner surface was sampled at ≥25% coverage. For this reason, the syringes used in subsequent experiments were imaged at 25% coverage.

Lastly, the automatic spot counting results were compared to the number from visual inspection for 200 randomly sampled images (Fig. 4) to determine the accuracy of the automatic algorithm. The size of the plotted point is proportional to the number of images with that particular spot count. Most of the images contained only a few spots. The dashed line (theoretical fit) shows the fit for one-to-one correspondence between the algorithm and visual inspection. Comparing the experimental fit to the theoretical fit, we see that the spot counting algorithm had a minor tendency to underestimate the manually determined number

of spots. On average, the estimated number of spots deviated from the manually determined number by less than 10%.

3.2. Association between Oil Distribution and Particle Counts

Fig. 5 shows the average distribution in heterogeneity along the barrel of the syringe. Both parameters had local maxima at roughly 20.3mm, 33.1mm, and 40.4mm from the starting position (dashed lines). There was also a sharp increase in each parameter value for locations beyond 44.0mm, close to the needle end of the syringe.

Fig 6 provides a comparison of the particle counts in PFS-F and PFS-D syringes. PFS-F syringes contained a high number of particle counts. In comparison to PFS-F syringes, PFS-D syringes exhibited significantly lower particle counts, as determined using the MFI™ instrument ($p < 0.001$, independent t-test). For both types of syringes, there were orders-of-magnitude more particles of smaller diameter.

Fig 7 provides sample interference fringes acquired from a PFS-F syringe and a PFS-D syringe. The sample interference image from the PFS-F syringe contains many fringes, indicative of a more uneven oil distribution. In comparison, the images acquired from PFS-D syringes tended to contain fewer fringes, and the fringes are of lower frequency; therefore, the oil distribution tends to be more slowly varying and even.

After quantifying the heterogeneity, the interferograms from PFS-D syringes were found to have significantly less number of spots and lower heterogeneity percent (Fig. 8; $p < 0.001$, independent t-test). In comparison to PFS-F, PFS-D syringes exhibited both significantly lower particle counts (Fig 6; $p < 0.001$) as well as significantly more homogeneous silicone oil layer distributions (Fig 8; $p < 0.001$) suggesting that a correlation could exist between silicone oil layer heterogeneity and particle counts.

To further determine whether there was an association between oil distribution and particle counts, Spearman’s rank correlation was computed between the average heterogeneity parameters and the particle counts (Table 1). The oil distribution was significantly correlated to particle counts, with stronger correlation for smaller particles. A Partial Correlation was also computed to account for possible effects due to syringe type (Table 1). After accounting for syringe type, Partial Correlation results show no significant association between oil distribution and particle counts.

4. Discussion

In this paper, we developed a technology to visualize and quantify the heterogeneity in the distribution of the silicone oil lining the inner surface of unfilled syringes. A multi-color interferometric imaging system was designed and built to visualize and quantify this silicone oil distribution. After evaluating the system’s repeatability and accuracy, the system was used in a preliminary investigation on the link between silicone oil distribution and particle formation. In this section, we will first discuss the system performance, followed by the results of the preliminary investigation.

Two parameters were chosen to quantify the silicone oil distribution heterogeneity from the acquired interference images: the number of spots, and the heterogeneity percent. The source of the dark spots are unknown. However, since silicone oil has high wettability [5], the oil distribution heterogeneity can imply the existence of impurities in the glass or other foreign particles that disturb the surrounding oil layer.

The data suggests that the parameters chosen can quantify the level of heterogeneity in the silicone oil distribution. For both parameters, the average parameter values along the barrel exhibited local maxima at the same positions and rose sharply near the needle end. The rise in heterogeneity at the needle end is not surprising - in cases where the silicone oil distribution is not even, the needle end tends to contain less silicone oil [3, 8, 10] and would be expected to be more uneven. Although the cause for the local maxima is unknown and requires further investigation, the agreement in both the number of occurrences and location along the barrel suggests that the parameters are measuring the same phenomenon.

The heterogeneity parameters are also repeatable: the coefficient of variation was less than 5% in both cases. One possible source for the variability is defocus: defocus decreases image contrast which negatively impacts the heterogeneity parameters. Since the coefficient of variation was below 5%, this variability was not considered to be a major issue.

Of the two parameters, the number of spots had a lower repeatability and a higher percent error when imaging at a smaller percent coverage. This is likely due to the discrete nature of the parameter: a spot will not be counted if it is not contained in the acquired images, or if the image is slightly defocused. This is distinct from the heterogeneity percent, which measures a continuous value calculated from the full field of view. Another point of consideration is that most images only contained a few spots, while very few images contained many spots. Images that contain a high number of spots, although uncommon, could heavily influence the average number of spots count for a syringe. The number of spots measured can become sensitive to sampling error when imaging at a lower percent coverage.

The percent error in estimating the heterogeneity when imaging only a small fraction of the inner surface area is high. To get a more accurate measure of the heterogeneity, at least 25% of the inner surface should be sampled. Conventional point-sampling reflectometry methods, which are typically used to measure the oil height at less than 1% of the inner surface, may not have sufficient sampling to accurately extrapolate properties about the oil distribution and its impact on syringe functionality and particle formation.

Overall, the system was able to visualize and quantify the heterogeneity in the silicone oil distribution within unfilled syringes over a large fraction of the inner surface area, up to 100%. As a method to quantify the evenness of the oil distribution, our method is complementary to other methods that focus on measuring other parameters, such as the global height distribution or the presence of silicone oil. Although we applied our system to syringes coated with silicone oil, our system can be used to characterize the distribution of other coatings as well. Our method can be beneficial in studies to investigate the impact of the oil distribution heterogeneity on syringe mechanical functionality or product particle

counts, and can be used complementarily to other methods due to its non-destructive nature. Apart from scientific studies, our method can also be helpful in syringe manufacturing in guiding new processes as well as screening supplies. While identifying the factors that contribute to the oil distribution heterogeneity is out of the scope of this study, one could speculate that factors may include particulates in the silicone oil used, particles from the manufacturing environment, silicone oil droplet size and distribution, and imperfections in the glass surface. Further studies may guide efforts to develop and manufacture better syringes.

We performed a preliminary investigation on the impact of the silicone oil distribution on particle formation. Our preliminary study involved two types of syringes, one of which was known to have higher particle counts. We found that PFS-D syringes contained significantly lower particle counts and homogeneous oil distributions in comparison to PFS-F syringes. However, within syringe types, no significant association was found.

There are many possible reasons for this lack of association that warrant further investigation. First, our study involved two types of syringes: PFS-F syringes and PFS-D syringes. There may be unaccounted differences between these two syringes that contributed to the variance in particle counts. For example, apart from the siliconization method, the syringe types also contain different amounts of silicone oil [19]. Factors such as silicone deposition method, silicone oil amount, and type of glass used for the barrel can impact particle formation [2, 5, 9, 20, 21].

Second, within each syringe type, the spread in the number of particles was not large. This would make finding an association difficult. A third source of variability is the extrusion: the number of particles formed during the extrusion process can vary depending on the extrusion force, the silicone oil layer thickness, and the fit between the barrel and stopper. Although the extrusion was performed using an Instron machine, tolerances in the dimensions of the syringe barrel and stopper could impact the total amount of silicone oil extruded through the needle and the force profile during extrusion, thereby adding variability in the number of particles formed.

Fourth, the measured particle counts can suffer from large sampling variability. The particle counts of larger diameter particles (≥ 10μm) were sometimes small. For example, the average number of particles per mL in PFS-D syringes was 200 and 3 for particles ≥10μm and ≥25μm respectively. Considering the sampling volume was about 0.5mL, the measurement of these low-concentration particles would have large sampling variability [22].

Our preliminary investigation did not show a significant association between oil distribution and particle counts. Further investigations that account for the aforementioned factors are required to more conclusively determine whether an interaction exists between particle counts and oil distribution.

5. Conclusion

In summary, we developed a new technology for visualizing and quantifying the heterogeneity in the distribution of silicone oil lining the inner surface of unfilled syringes and applied our system in a preliminary study investigating the impact of silicone oil distribution on particle formation. Between syringe types, there was a strong association between particles counts and oil distribution. No association between particle counts and oil distribution was found within syringe types; however, there are many sources of variability that bear additional investigation. Since the percent error is large for small percent coverages, studies looking into the oil distribution heterogeneity should involve methods that can cover at least a moderate fraction of the inner surface. Our system will be beneficial in future investigations that study the impact of the distribution of silicone oil, or other lubricants, on particle formation and functionality in pre-filled syringes and can be useful as a feedback mechanism for guiding the development of better syringe manufacturing processes as well as a quality control tool to screen incoming syringe supplies.

Acknowledgements

This work was supported by Amgen (2016740555). M. Cua acknowledges the support from the Natural Sciences and Engineering Research Council of Canada (NSERC). D. Martin acknowledges the support from the Predoctoral Biotechnology Leadership Training from the National Institute of Health (NIH 1T32GM112592) and the Donna and Benjamin M. Rosen Bioengineering Center Fund (9900050).

Abbreviations used:

MFI	microflow imaging
PFS	prefilled syringe
PFS-F	prefilled syringe – fixed nozzle
PFS-D	prefilled syringe – diving nozzle
SbVP	sub-visible particles

References

[1]. Makwana S, Basu B, Dharamsi A, Prefilled syringes: An innovation in parenteral packaging, International Journal of Pharmaceutical Investigation 1 (4) (2011) 200–206.

[2]. Felsovalyi F, Janvier S, Jouffray S, Soukiassian H, Mangiagalli P, Silicone-Oil-Based Subvisible Particles: Their Detection, Interactions, and Regulation in Prefilled Container Closure Systems for Biopharmaceuticals, Journal of Pharmaceutical Sciences 101 (12) (2012) 4569–4583.

[3]. Wen ZQ, Vance A, Vega F, Cao X, Distribution of Silicone Oil in Prefilled Glass Syringes Probed with Optical and Spectroscopic Methods, PDA Journal of Pharmaceutical Science and Technology 63 (2) (2009) 149–158.

[4]. Jones LS, Kaufmann A, Middaugh CR, Silicone oil induced aggregation of proteins, Journal of Pharmaceutical Sciences 94 (4) (2005) 918–927.

[5]. Gerhardt A, Nguyen BH, Lewus R, Carpenter JF, Randolph TW, Effect of the siliconization method on particle generation in a monoclonal antibody formulation in pre-filled syringes, Journal of Pharmaceutical Sciences 104 (5) (2015) 1601–1609.

[6]. Corvari V, Narhi LO, Spitznagel TM, Afonina N, Cao S, Cash P, Cecchini I, DeFelippis MR, Garidel P, Herre A, Koulov AV, Lubiniecki T, Mahler HC, Mangiagalli P, Nesta D, Perez-

Ramirez B, Polozova A, Rossi M, Schmidt R, Simler R, Singh S, Weiskopf A, Wuchner K, Subvisible (2-100 μm) particle analysis during biotherapeutic drug product development: Part 2, experience with the application of subvisible particle analysis, Biologicals 43 (6) (2015) 457–473.

[7]. Krayukhina E, Yokoyama M, Hayashihara KK, Maruno T, Noda M, Watanabe H, Uchihashi T, Uchiyama S, An assessment of the ability of submicron-and micron-size silicone oil droplets in dropped prefillable syringes to invoke early-and late-stage immune responses, Journal of Pharmaceutical Sciences 108 (7) (2019) 2278–2287.

[8]. Loosli V, Germershaus O, Steinberg H, Dreher S, Grauschopf U, Funke S, Methods to determine the silicone oil layer thickness in sprayed-on siliconized syringes, PDA journal of pharmaceutical science and technology (2018) 278–297.

[9]. Funke S, Matilainen J, Nalenz H, Bechtold-Peters K, Mahler HC, Friess W, Silicone Migration From Baked-on Silicone Layers. Particle Characterization in Placebo and Protein Solutions, Journal of Pharmaceutical Sciences 105 (12) (2016) 3520–3531.

[10]. Eu B, Cairns A, Ding G, Cao X, Wen Z-Q, Direct visualization of protein adsorption to primary containers by gold nanoparticles, Journal of pharmaceutical sciences 100 (5) (2011) 1663–1670.

[11]. USP, Particulate Matter in Injections, in: United States Pharmacopeia and National Forumlary (USP 41 - NF 36), 2018, Ch. <788>.

[12]. JP, Foreign Insoluble Matter Test for Injections, in: The Japanese Pharmacopoeia 17th Ed., 2016, Ch. 6.06. URL http://www.pmda.go.jp/english/pharmacopoeia/pdf/jpdata/JP16eng.pdf

[13]. EP, Particulate contamination: sub-visible particles, in: European Pharmacopoeia, 2016, Ch. 2.9.19.

[14]. Carpenter JF, Randolph TW, Jiskoot W, Crommelin DJ, Middaugh CR, Winter G, Ying-Xin FA, Kirshner S, Verthelyi D, Kozlowski S, Clouse KA, Swann PG, Rosenberg AM, Cherney B, Overlooking subvisible particles in therapeutic protein products: Gaps that may compromise product quality, Journal of Pharmaceutical Sciences 98 (4) (2009) 1201–1205.

[15]. Bukofzer S, Ayres J, Chavez A, Devera M, Miller J, Ross D, Shabushnig J, Vargo S, Watson H, Watson R, Industry Perspective on the Medical Risk of Visible Particles in Injectable Drug Products, PDA Journal of Pharmaceutical Science and Technology 69 (1) (2015) 123–139.

[16]. Funke S, Matilainen J, Nalenz H, Bechtold-Peters K, Mahler H-C, Friess W, Analysis of thin baked-on silicone layers by ftir and 3d-laser scanning microscopy, European Journal of Pharmaceutics and Biopharmaceutics 96 (2015) 304–313.

[17]. Santos A, Ortiz de Sol'orzano C, Vaquero JJ, Pena J, Malpica N, Del Pozo F, Evaluation of autofocus functions in molecular cytogenetic analysis, Journal of microscopy 188 (3) (1997) 264–272.

[18]. Quiroga JA, Servin M, Marroquin JL, Regularized phase tracking technique for demodulation of isochromatics from a single tricolour image, Measurement Science and Technology 13 (1) (2002) 132–140.

[19]. Wright J, Soukiassian H, Prefillable Syringe Technology - BD Neopak- Delivering the Next Generation in Glass Prefillable Syringes, https://drug-dev.com/prefillable-syringe-technology-bd-neopak-delivering-the-next-generation-in-glass-prefillable-syr [Online; accessed 22-March-2020] (2014).

[20]. Depaz RA, Chevolleau T, Jouffray S, Narwal R, Dimitrova MN, Cross-linked silicone coating: a novel prefilled syringe technology that reduces subvisible particles and maintains compatibility with biologics, Journal of pharmaceutical sciences 103 (5) (2014) 1384–1393.

[21]. Wang C, Cheong FC, Ruffner DB, Zhong X, Ward MD, Grier DG, Holographic characterization of colloidal fractal aggregates, Soft Matter 12 (42) (2016) 8774–8780.

[22]. Ríos Quiroz A, Lamerz J, Da Cunha T, Boillon A, Adler M, Finkler C, Huwyler J, Schmidt R, Mahler HC, Koulov AV, Factors Governing the Precision of Subvisible Particle Measurement Methods - A Case Study with a Low-Concentration Therapeutic Protein Product in a Prefilled Syringe, Pharmaceutical Research 33 (2) (2016) 450–461.

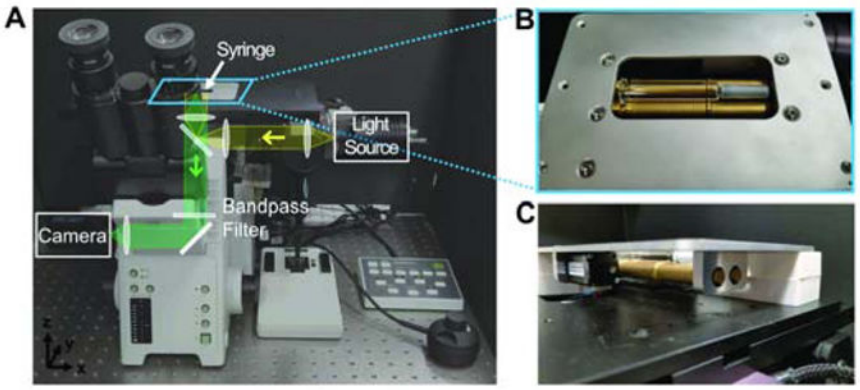

Figure 1: Overview of the Multi-Color Interferometric Imaging System.

(A) A photo of the imaging system, consisting of a modified, inverted, reflected-light microscope, motorized stage, and syringe holder. A simplified 2D schematic of the optical setup has been provided, with the main components of the illumination (shown in yellow) and detection (shown in green) light paths overlaid. The coordinate system is shown on the bottom left. (B) Zoomed-in view of the customized holder for 2.25mL syringes. The syringe rests on two rods that rotate. (C) Side view of the syringe holder.

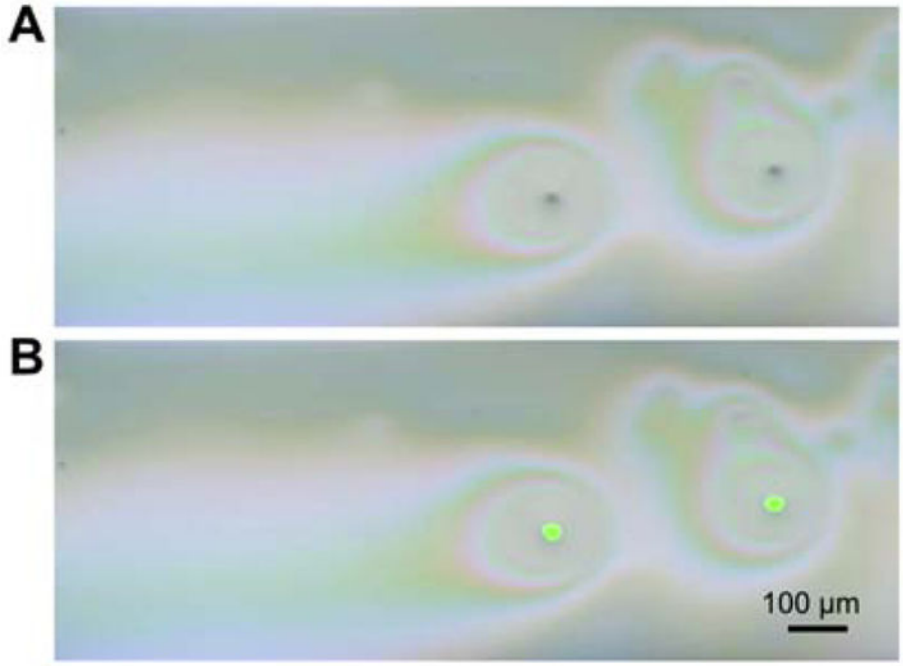

Figure 2: Automatic Detection of Dark Spots in an Interferogram.

(A) An example of an interferogram with dark spots at the center of two circular fringe patterns. (B) Automatic detection of dark spots (highlighted in green) using an image processing method. Finding the number of dark spots at the center of fringes is one method for quantifying the heterogeneity in the oil distribution.

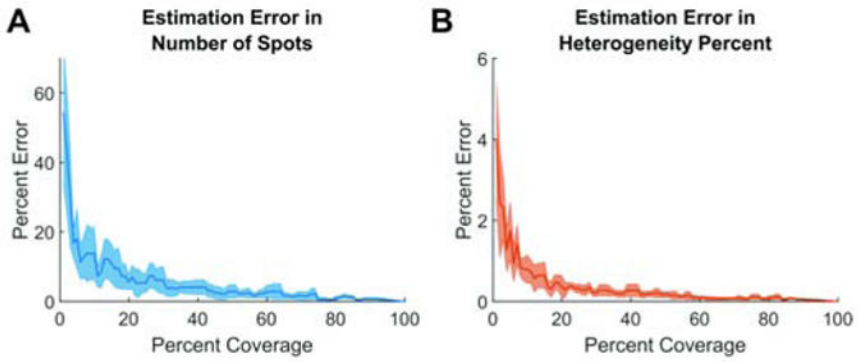

Figure 3: Impact of Imaging at Lower Percent Coverage.

The percent error in estimating the silicone oil distribution heterogeneity when imaging at a lower percent coverage is shown for (A) the number of spots and (B) the heterogeneity percent. The shaded error bar shows twice the standard error of the mean.

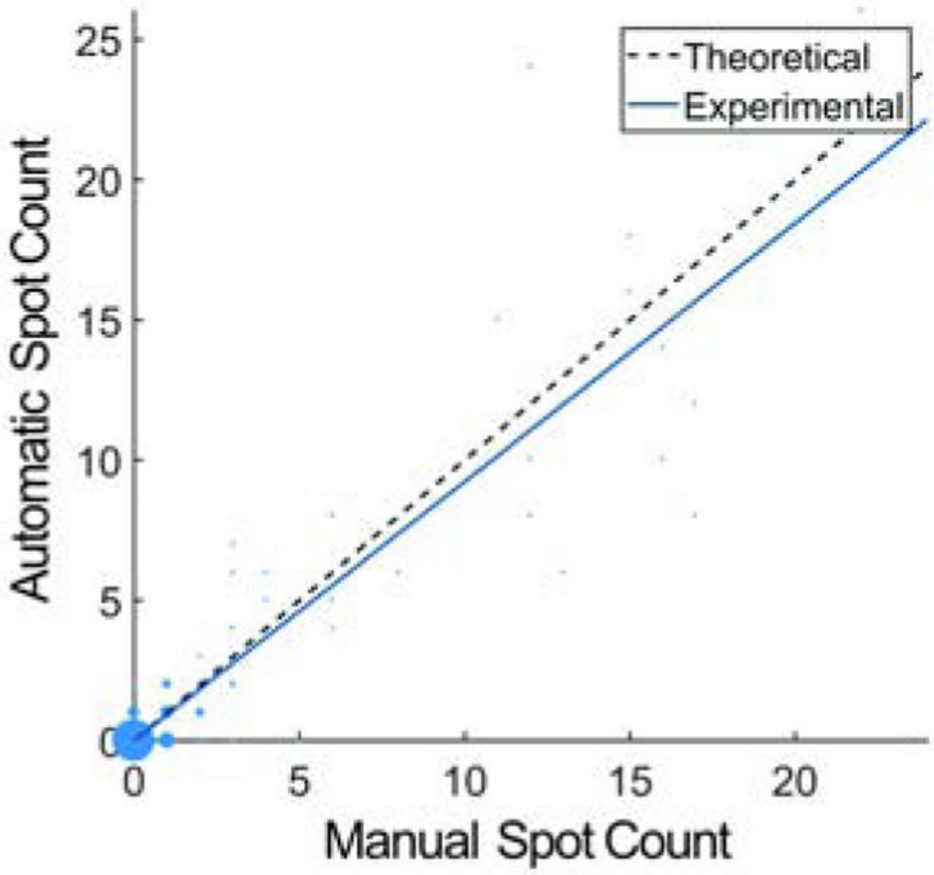

Figure 4: Comparison of Manual versus Automatic Spot Counting.

The plot compares the number of spots counted automatically versus manually, via visual inspection. The area of each point is proportional to the number of images satisfying that data point. The theoretical fit shows the expected fit for a one-to-one correspondence. The automatic spot counting algorithm has a minor tendency to underestimate the number of spots.

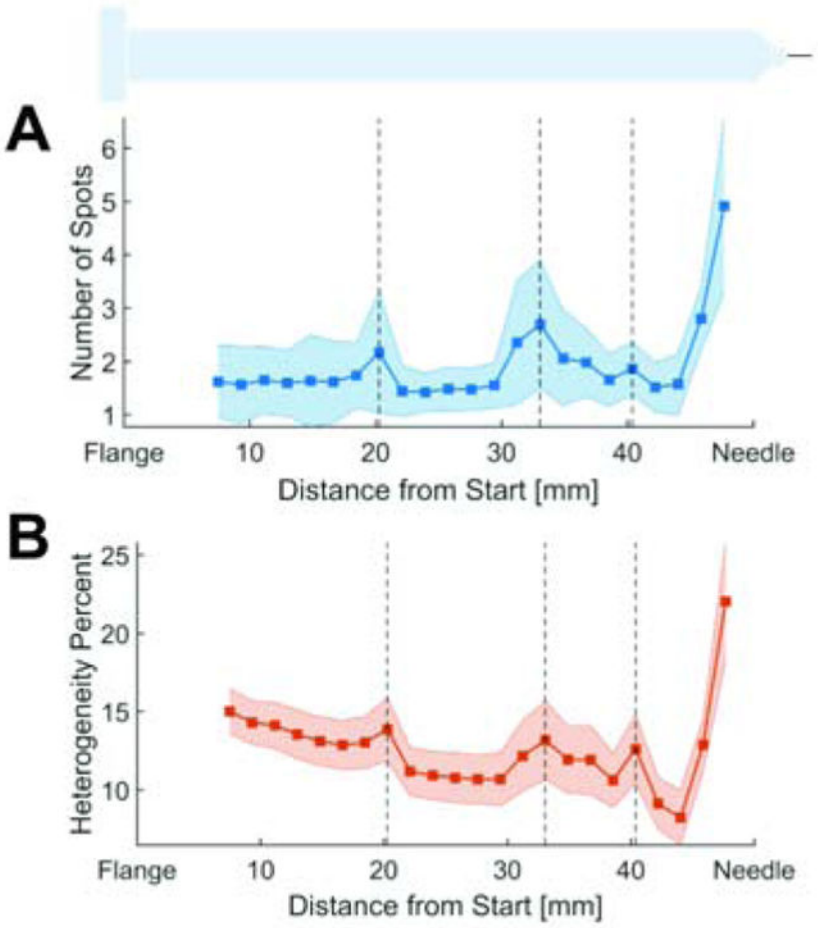

Figure 5: Spatial Distribution of Heterogeneity.

The average distribution of heterogeneity along the syringe barrel was computed for (A) the number of spots and (B) the heterogeneity percent. The shaded areas are +/− two times the standard error of the mean. The dashed lines highlight the local maxima measured by all the parameters.

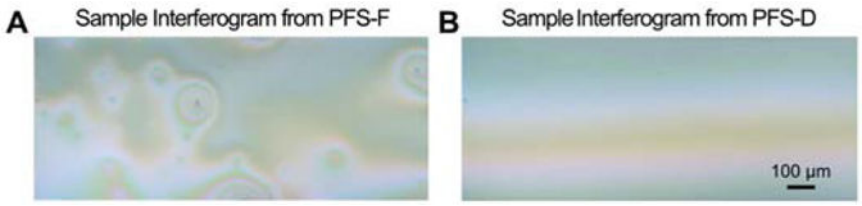

Figure 6: Comparison of particle counts in PFS-F and PFS-D syringes.

PFS-D syringes contain significantly lower particle counts than PFS-F syringes, for particles of size (A) ≥1µm, (B) ≥10µm, and (C) ≥25µm.

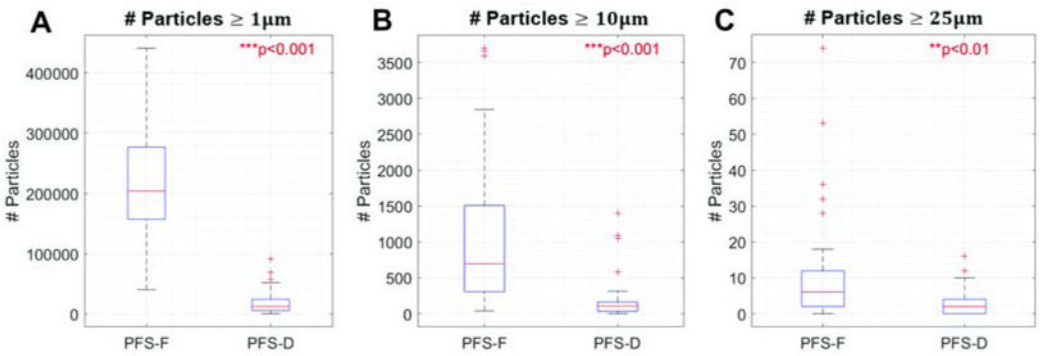

Figure 7: Sample interferograms from a PFS-F syringe and a PFS-D syringe.

Representative interference images from PFS-F syringes (A) and PFS-D syringes (B) show the difference in silicone oil distribution between the two syringe types. Images acquired from PFS-F syringes tended to contain more fringes, indicative of a more heterogeneous oil distribution. In comparison, images from PFS-D syringes tended to contain fewer fringes, and the fringes were of lower frequency, implying that the oil distribution in PFS-D syringes were more slowly varying and even.

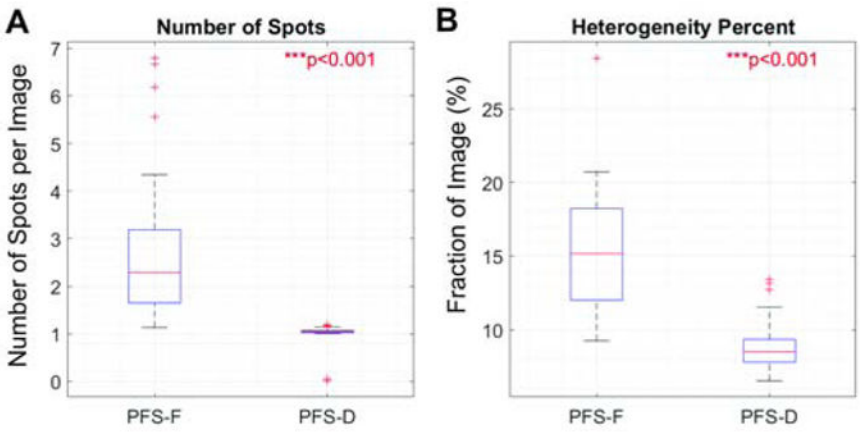

Figure 8: Comparison of silicone oil distribution heterogeneity in PFS-F and PFS-D syringes.

The heterogeneity in the oil distribution was quantified using (A) the number of spots, and (B) the heterogeneity percent. The oil distribution in PFS-D syringes were significantly less heterogeneous (had lower number of spots and lower heterogeneity percent) in comparison to PFS-F syringes.

Table 1:

Correlation Results Investigating Association between Cumulative Particle Counts and Heterogeneity Measures.

Bi-variate Spearman correlation between particle counts and heterogeneity measures shows significant association. Partial correlation accounting for syringe type shows no significant association.

Particle Size	Spearman Correlation r_s		Partial Correlation r_s	
	Number of Spots	Het. Percent.	Number of Spots	Het. Percent
≥ 1 μm	0.74***	0.69***	0.15	0.01
≥ 2 μm	0.74***	0.70***	0.07	−0.08
≥ 5 μm	0.71***	0.70***	−0.05	−0.08
≥ 10 μm	0.54***	0.55***	−0.11	0.07
≥ 25 μm	0.34**	0.27**	−0.05	−0.10

Significant correlations reported as

** $p < 0.01$

*** $p < 0.001$.